Modelling Simul. Mater. Sci. Eng. 1 (1993) 731–740. Printed in the UK

Molecular-dynamics simulations of low-energy copper atom interaction with copper surfaces

S P Chou and N M Ghoniem

Mechanical Aerospace and Nuclear Engineering Department, University of California, Los Angeles, Los Angeles, California 90024-1597, USA

Received 6 January 1993, accepted for publication 2 March 1993

Abstract. The interaction between low-energy copper atoms and an atomically smooth [100] copper surface is investigated using a molecular-dynamics (MD) computational method. A newly formulated interatomic potential, which empirically combines the Ziegler universal potential at high energy and the embedded-atom many-body potential at low energies, is utilized in the study of near-surface cascade dynamics. The analysis includes sputtering of surface atoms, and reflection and penetration of incident Cu atoms. It is shown that the sputtering yields of low-energy Cu atoms on a [100] Cu surface are in general agreement with the experiments of Hayward and Wolter and with other MD calculations performed by Shapiro and Tombrello using only pair potentials. However, in contrast with pair-potential-type calculations, and in agreement with experimental observations, our work shows a smooth transition from reflection to adsorption as the incident atom energy is lowered. Detailed mechanisms of sputtering and reflection of atoms with energies in the range 10–1000 eV are given.

1. Introduction

In many technological applications, detailed knowledge of low-energy atom interaction with surfaces is required. Emphasis in recent years has been on material processing technologies, such as with ion beams, and the interaction of low-energy plasmas with surfaces. A fundamental understanding of the mechanistic process which influence such dynamic interactions is necessary. It is now appreciated that analytical transport theories [1, 2] break down in this low-energy regime. Methods based on the binary-collision approximation (BCA) are generally questionable at low incident–particle energies. A number of computer programs have been developed for the study of ion–solid interactions (e.g. the TRIM [3] and TRIPOS [4, 5] codes), and the results are in agreement with many experiments at high incident atom energies. The validity of these Monte Carlo (MC) computer programs is not justified at low energies, mainly because of their use of a BCA.

Therefore, and in order to gain insight into the physical mechanisms responsible for ion–surface interaction at low energies, molecular dynamics (MD) methods are preferred. Nevertheless, since the calculations represent the solution of a deterministic dynamical problem, the results will depend on both initial and boundary conditions. Another important factor in the details of cascade dynamics is the description of the interatomic potential. In this paper, we address these concerns by presenting a comprehensive and detailed study of the interaction (e.g. reflection, penetration and sputtering) of Cu atoms, incident with energies in the range 10–1000 eV, with a [100] Cu surface.

The interaction of energetic Cu ions with the [100] Cu surface, up to 600 eV, has been experimentally studied by Hayward and Wolter [6]. Their results indicate that the sputtering

0965-0393/93/050731+10$07.50

threshold is in the neighbourhood of 60 eV and that its value increases to about three for the highest energy studied. Shapiro and Tombrello [7] used an MD technique to contact a numerical simulation of the sputtering process. In their study, the interatomic potential is composed of two pure pair potentials, namely the Born–Mayer and the Morse. Their results are in reasonable agreement with the experimental sputtering yield data, although they generally give an overestimate.

The absence of any reflected atoms in the computer simulations of Shapiro and Tombrello is at variance with experimental data [8, 9], although they discussed four different possibilities for the lack of agreement with experiments. We will demonstrate here that the primary source of discrepancy is a result of the pair-wise nature of their interatomic potential. Earlier results of Jakas and Harrison [10] identified the importance of 'correlated motion' of sputtered atoms in what was termed a multiple-interaction (MI) model, for contrast with BCA simulations. However, their use of pure pair potentials (a combination of Thomas–Fermi–Molier and Morse) precluded direct conclusions on the effects of the many-body aspects of interatomic potentials. More recently, Garrison *et al* [11, 12] demonstrated the importance of many-body interactions for describing the energy- and angle-resolved distributions of neutral Rh atoms ejected from keV-ion-bombardment Rh{111}. They showed that the most dramatic difference between the many-body potential and the pair potentials is the predicted kinetic-energy distribution of ejected atoms. In agreement with experiments, their results show a broader peak at ~4 eV for the many-body case, as compared to a narrower peak at 2 eV for pair-wise simulations. Reimann *et al* [13] (using many-body/pair potentials for Rh, and a pure pair potential for O) showed that the peak in energy distribution of Rh atoms from the O-covered surface is at a lower energy value than that of the clear metal. They concluded that collisional energy-loss processes contribute to determining the peak position as well as the well known binding-energy effect.

Harrison and co-workers (see, e.g., [14–16]) analysed many features of the interaction between low-energy impinging ions and various substrates. However, the representation of interatomic potentials in their work is of the pair-wise type, which does not account for the local environment that the atom experiences through the many-body potential. Other computer simulations which utilise the EAM in constructing interaction potentials, such as those of Smith and co-workers [17] and Maboudian *et al* [18], have direct relevance to the work reported in this paper.

Recently, we developed and used a new computer code, CASC-MD, for the study of low-energy atomic collision phenomena in solids [19, 20]. A composite potential, which is of the pair type at high energies and the many-body at low energies, is used in CASC-MD. Low-energy bulk cascade dynamics are shown to give the correct displacement threshold surface in the bulk of a Cu single crystal. The intent of this paper is to extend our earlier work to the study of the interaction of 10–1000 eV normally incident Cu atoms with a [100] Cu surface. In section 2, we summarize the theoretical background of our method and in section 3, relevant aspects of the computational technique are outlined. Results for near-surface cascade dynamics, sputtering, reflection, implantation and adsorption are presented in section 4. Finally, the conclusions of this work are given in section 5.

2. Theoretical background

In reference [20], we give details of the development of a composite pair/many-body potential for Cu. We also describe our numerical technique for the integration of the equations of motion (EOMs), and the particular treatment of atoms at the boundary of a

computational cell. While the interested reader should consult [20] for more details, we will briefly describe our approach here for the sake of self-consistency.

In our work, Ziegler's universal potential [21] is selected to describe pair atomic interactions at high energies, while an approximation to the EAM potential is used for the description of many-body interactions at low energies. For the intermediate-energy regime, a cubic-spline potential is used to allow for the continuity of this composite potential throughout the entire energy range. Ziegler's pair potential for high-energy binary interactions has the form [21]

$$\phi_Z(R_{ij}) = \frac{Z_i Z_j e^2}{R_{ij}} \sum_{k=1}^{4} C_i \exp(-b_k R_{ij}/a_0) \tag{1}$$

where Z_i and Z_j are the atomic numbers of the interacting particles i and j, respectively, and R_{ij} is their separation distance; e is the electron charge; C_k and b_k are constants; and a_0 is the screening length [21].

The approximation of the low-energy many-body EAM was first derived by Foiles [22], on the basis of the EAM framework originally developed by Daw *et al* [23, 24]. The potential has the form

$$\Phi_{EAM}(R_{ij}) = \phi_{ij}(R_{ij}) + 2[\partial F_i(\rho^a)/\partial\rho]\rho_{ij}^a(R_{ij}) + [\partial^2 F_i(\rho^a)/\partial\rho^2][\rho_{ij}^a(R_{ij})]^2 \tag{2}$$

where F_i is the embedding function for atom i, $\rho_{ij}^a(R_{ij})$ is the average local electron-density contribution from atom j on atom i at a separation distance of R_{ij}, ϕ_{ij} is the core–core pair repulsive potential between interacting atoms i and j, and ρ^a is the total average local electron density from all atoms in the neighbourhood of atom i.

A transitional cubic-spline potential which bridges the Ziegler and EAM potentials is assumed to have the form

$$\Phi_s(R_{ij}) = \sum_{k=0}^{3} d_k R_{ij}^k \tag{3}$$

where d_k are splitting constants.

Any selection of potential boundaries r_1 and r_2 should guarantee continuities of potential and force (potential gradient). However, a proper selection of potential boundaries can reduce the degree of drastic gradient changes in the potential because it is only piece-wise continuous. The interaction of two atoms at a separation r is then completely described by the composite potential of the form

$$\Phi(R_{ij}) \begin{cases} \Phi_Z(R_{ij}) & 0 < R_{ij} \leqslant r_1 \\ \Phi_s(R_{ij}) & r_1 \leqslant R_{ij} \leqslant r_2 \\ \Phi_{EAM}(R_{ij}) & r_2 \leqslant R_{ij} \leqslant r_c \end{cases} \tag{4}$$

where r_c is the cutoff distance (~5.0 Å) for the low-energy many-body potential.

It is noted that Φ_{EAM} is derived from the EAM description of atomic interactions, and, strictly speaking, is valid in regions where the variation in the average electron density is small. The full EAM description is shown to be necessary for many near-equilibrium surface phenomena. However, since our analysis is restricted to incident atom energies above 10 eV, Φ_{EAM} is a reasonable approximation. If higher accuracy is required for energies below 10 eV, the full EAM description should be used.

For Cu, the optimum values of r_1 and r_2 were found to be 1.5 and 2.0 Å, respectively. The spline potential is not only a function of the interatomic separation, but also a function of the total average local electron density. For instance, near-surface atoms sit in different average local electron density, as compared to bulk atoms, because of the neighbouring atom configurations.

3. Computational technique

Although the MD method is a powerful tool to investigate atomistic processes, particularly those that are related to the crystal structure and the interatomic potential, it is known to have two main drawbacks. First, the results are sensitive to the size and boundary conditions of the computational cell. Second, the details of the dynamics are dependent upon the initial configuration (i.e., the initial conditions).

We have developed a computational technique for the treatment of boundary atoms [20]. In this technique, we modify the EOMs for boundary atoms by the introduction of a fictitious viscosity μ, an effective spring constant κ, and a net balancing force F_b. In this manner, the computational cell, which is embedded in a visco-elastic solid, does not result in energy reflection at its boundaries. The fictitious viscosity is chosen so as to produce an energy damping time constant smaller than the cascade transit time within the computational cell. This procedure solves, in a satisfactory way, the problem of boundary conditions, although it is not rigorously consistent with continuum mechanics. It is worth noting that periodic boundary conditions are not appropriate here, since ion–solid interaction problems involve statistical systems which are far from thermodynamic equilibrium. The second weakness, that is, the effect of initial conditions, presents itself when some sampled parameters of the calculations are of particular interest (e.g., the probabilities of sputtering, reflection and implantation per incident atom). Statistical sampling (or biasing) techniques are highly dependent on the desired estimator. Since we are interested in more than one estimator (e.g., sputtering, reflection, and implantation), we choose here to use a simple uniform sampling technique, as shown below.

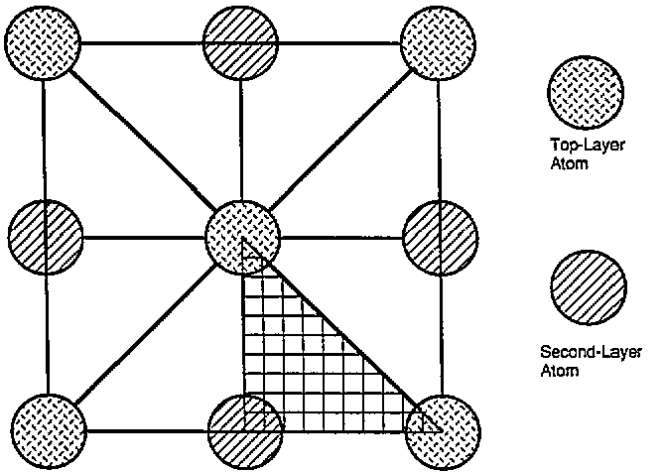

Figure 1. Representation of a unit cell surface on the [100] plane for Cu.

On the [100] surface, a unit cell has an eightfold symmetry, as shown in figure 1. The computations take advantage of this symmetry and consider only one of the symmetrical zones. We distribute the normally incident atoms uniformly over this basic areal unit, which is further divided into 55 regions. Of these small areas, 45 are squares (0.033 $Å^2$) while the remaining ten are triangles (0.016 $Å^2$), as shown in figure 1. With each of these 55 areas, a random-number generator is used to locate the initial position of the impacting ion. A weighting factor of 0.5 is used for results obtained from the triangular areas. Thus, we believe our calculations to be statistically significant, although larger samples would necessarily reduce the uncertainty in the average values of calculated parameters.

The truncation of the solid to create the [100] surface results in an initial relaxation of the first surface layer. Relaxation calculations are first performed at 300 K to produce the equilibrium configuration of the atoms in the computational cell, including surface atoms. The system size is determined on the basis of the incident atom energy. For a typical simulation of 100 eV incident atoms, the number of atoms in the computational cell is 761, and the number of boundary atoms is 829, giving a total of 159 × 6 EOMs, including the incident atom. A typical computer run simulating the system dynamics up to 1 ps takes about 700 CPU s on the CRAY-2 super-computer.

4. Results

The sputtering yield as a function of incident atom energy is shown in figure 2, together with the experimental data of Hayward and Wolter [6], and the MD simulations of Shapiro and Tombrello [7]. Since the results of our calculations and those of Shapiro and Tombrello both agree with the experimental data (within experimental and numerical uncertainties), and since we use different interatomic potentials, it is concluded here that sputtering yield measurements cannot be of great value to the determination of the structure of the interatomic potentials at low energies. Although our composite pair/many-body potential is sufficiently different from the Born–Mayer/Morse composite potential used by Shapiro and Tombrello, both calculations are more or less in agreement with experiments. However, fundamental differences seem to exist in calculations of the reflection and implantation profiles, as will be discussed later.

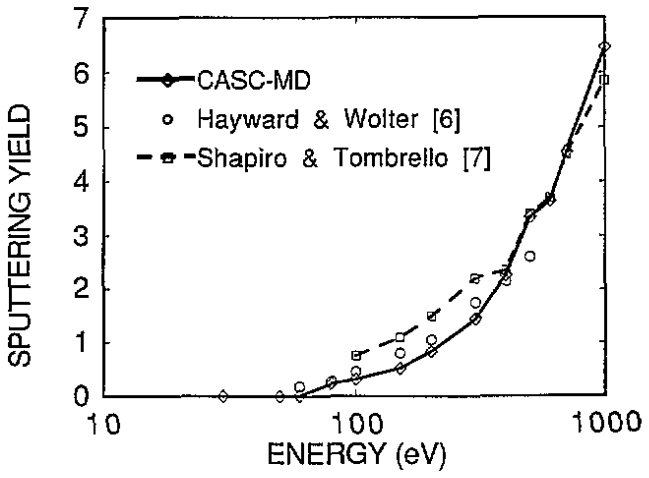

Figure 2. Comparison of the results from CASC-MD sputtering-yield calculations as a function of energy with those from experiments [6] and calculations [7].

To further clarify the sputtering mechanisms in the energy range 10–1000 eV, regions of inhibited sputtering (shaded areas) on a unit cell surface are shown in figure 3 for low energy (80 and 150 eV), and in figure 4 for high energy (500 and 1000 eV). The contrast between the inhibited-sputtering mechanisms operating at both low and high energies can be understood as follows. At low energies, regions of inhibited sputtering yields are directly on top, and in the immediate vicinity, of surface atoms. Linear replacement-collision-sequence (RCA) chains are formed, thus dissipating the incident atom energy deep into the solid. Very little energy is left at the surface to cause sputtering events. Regions of inhibited sputtering are larger over the top of second-layer surface atoms, because incident atoms lose part of

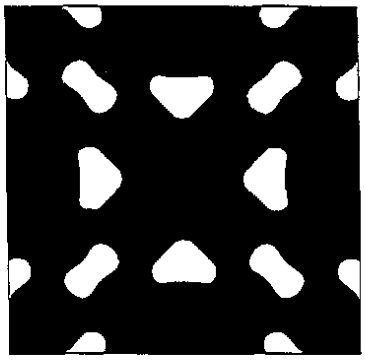

(A)

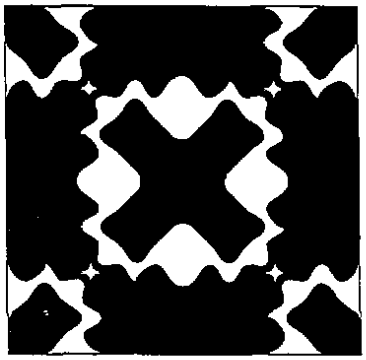

(B)

Figure 3. Regions of inhibited sputtering (shaded areas) on a [100] unit cell surface at low incident atom energies of (*a*) 80 and (*b*) 150 eV.

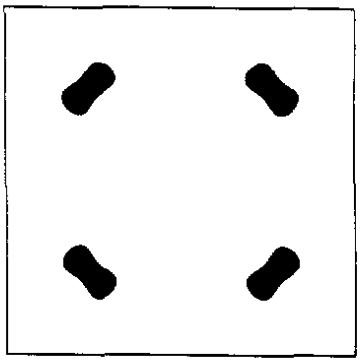

(A)

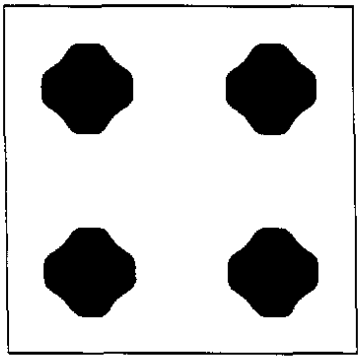

(B)

Figure 4. Regions of inhibited sputtering (shaded areas) on a [100] unit cell surface at high incident atom energies of (*a*) 500 and (*b*) 1000 eV.

their energy penetrating the first surface layer. Sputtering zones for low-energy atoms are found to be centred around channelling directions. Low-energy atoms do not penetrate deep into the solid so their energy is dissipated close to the surface when they proceed in a channel. Surface recoils are produced and thus sputtering ensues.

The sputtering mechanism at high incident atom energies is quite distinct from the low-energy mechanism explained above. If energetic atoms fall into a channel, they generally penetrate, leaving little energy to cause sputtering at the surface. Figure 5 illustrates this process. The trajectories of atoms within the entire computational cell are plotted, showing the familiar channeling process by a 500 eV incident Cu atom.

In figure 6, we show the trajectories of atoms during a low-energy sputtering (60 eV), while in figure 7, the mechanism of multiple sputtering is illustrated for an incident Cu atom with an energy of 500 eV. It is observed that only the backward-recoiling atoms that succeed in overcoming the attractive forces of the surface are sputtered. Other atoms first detach and then attach. Because such events are sensitive to the structure of the potential near the surface, the importance of an accurate many-body potential is apparent.

An important aspect of the analysis of sputtering mechanisms is the depth of origin of sputtered atoms. As expected, the majority of sputtered atoms originate from the first atomic surface layer. However, as the incident atom energy is increased, a greater fraction of atoms originate from deeper layers. Our results indicate that all sputtered atoms originate from the first surface layer for an incident energy up to about 100 eV. The fraction of sputtered atoms originating from layers below the first layer is about 5% at 500 eV and climbs up to

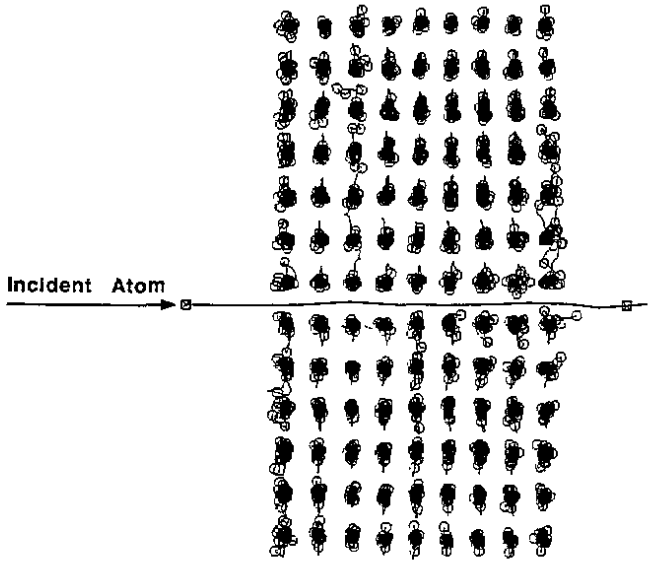

Figure 5. Atom trajectories during a channeling event. The incident atom has an energy of 500 eV.

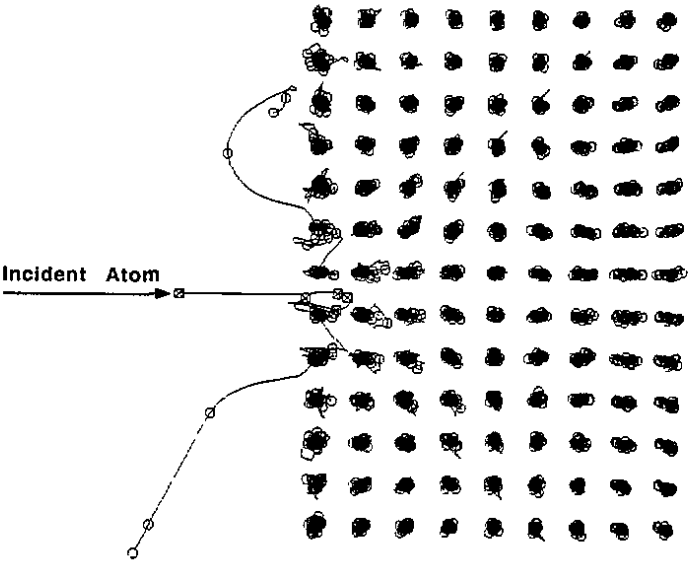

Figure 6. Atom trajectories during a low-energy (60 eV) sputtering event.

about 20% at 1000 eV.

The reflection coefficient as a function of incident atom energy is shown in figure 8. As indicated earlier, while the MD results of Shapiro and Tombrello apparently give no reflection of incident Cu atoms, our calculations show that Cu atoms with energies up to about 300 eV are all adsorbed or implanted, while above 300 eV reflection increases as a function of incident atom energy. Calculations from the binary-collision MC code (TRIM) are shown for contrast. It is clear from this comparison that MD simulations with many-body effects result in a more physical dependence of the reflection coefficient. Our results indicate that a transition occurs from adsorption at low energies to reflection at high energies. It is to be noted that this transition occurs at lower energy for low-Z incident atoms. The shift in adsorption-to-reflection transition energy with the incident atom charge is caused by a

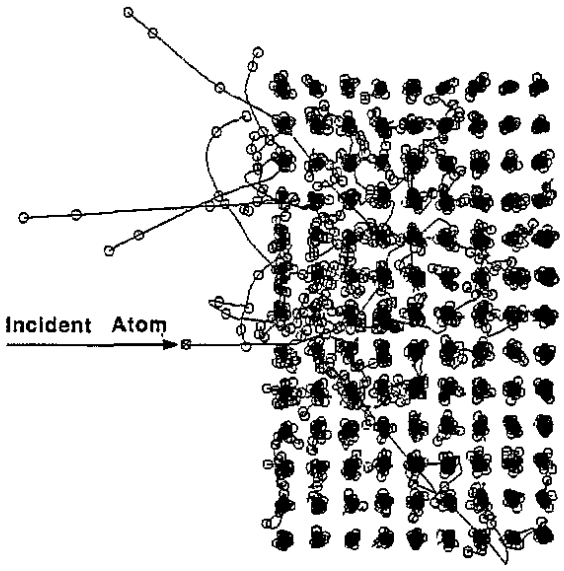

Figure 7. An example of multiple sputtering of Cu surface atoms for an incident atom energy of 500 eV.

larger interaction cross section and large electronic stopping powers for higher-Z atoms. Thus, high-Z atoms lose their energy at a faster rate and are more readily adsorbed. The binary-collision TRIM code calculations cannot reproduce the transition from reflection to adsorption as the energy of the incident particle is lowered, because the form of the potential used in TRIM is repulsive. Even if attractive terms are added to the interatomic potential, the results are apt to be inaccurate. This is mainly because many-body effects must be accurately considered in the low-energy range. Numerous experiments on energetic ion deposition are based on sufficient condensation (i.e., low reflection) at low energies [25–27].

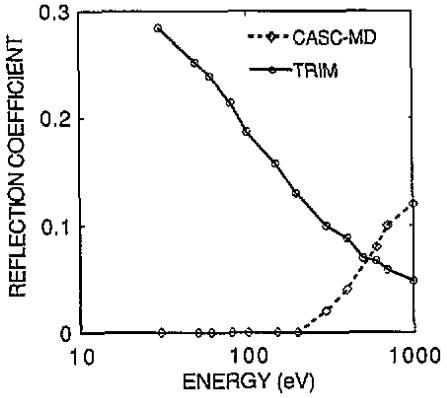

Figure 8. Dependence of the reflection coefficient on the incident Cu energy from TRIM and CASC-MD simulations.

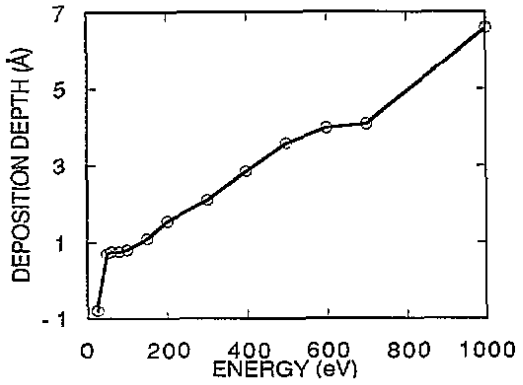

Figure 9. Dependence of the deposition depth of incident Cu atoms on their energy.

Reflection events take place only for high-energy near-head-on collisions. Only with these types of collision will the incident atom be drastically deflected so that it remains near the surface. A number of additional collisions will then occur which collectively result in the incident atom overcoming the surface binding potential (in order for that atom to

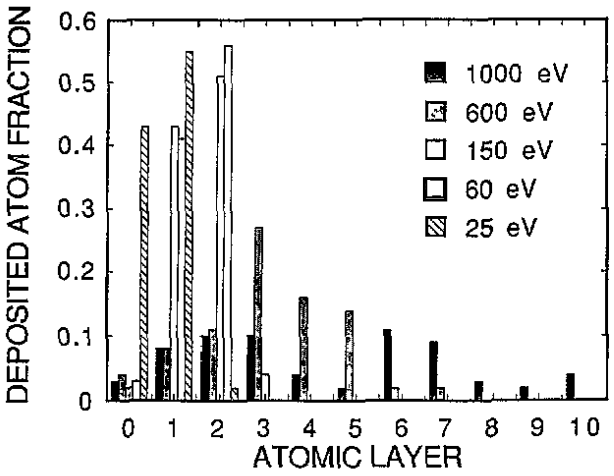

Figure 10. Fraction of deposited atom per atomic layer for various incident atom energies.

be reflected). For low-energy atoms, RCAs reduce the incident atom energy, resulting in surface adsorption.

Implantation of incident atoms is illustrated in figures 9 and 10. The average implantation depth as a function of the incident atom energy is shown in figure 9. The top surface is labelled as '1'. The layer labelled '0' is mainly composed of atoms which are not energetic enough to penetrate into the solid and are adsorbed, therefore, on the top surface. It is noted that for very low energies (e.g. 25 eV), a relatively large portion of incident atoms is adsorbed on top of the first surface atomic layer (in layer '0'). The deposition depth of implanted atoms at various incident atom energies is shown in figure 10.

5. Summary and conclusions

A comprehensive study of Cu atom interaction with the [100] Cu surface has been performed. It is concluded that the composite pair/many-body potential results in good agreement with the experimental sputtering yield data. The following results are shown.

(1) At low incident atom energies, regions of inhibited sputtering occur in the vicinity of efficient-energy-transfer directions (i.e. directly on top of surface atoms).

(2) Inhibited sputtering at high incident atom energies is associated with the phenomenon of channeling.

(3) The many-body part of the interatomic potential is significant for atomic events of multiple attachment and detachment of surface atoms.

(4) Only a very small fraction of sputtered atoms originate from atomic layers deeper than the first surface layer. This is about 5% up to 500 eV and increases to about 20% at 1000 eV.

(5) Reflection of energetic Cu atoms from the [100] Cu surface is demonstrated. The reflection coefficient increases monotonically up to about 12% at 1000 eV, with a threshold energy of about 200 eV.

(6) The implantation profile and depth distribution of incident atoms are uncharacteristically Gaussian. At lower energies, atom deposition is mainly in the first few atomic layers. However, a significant fraction of high-energy atoms channel through the surface resulting in broad distributions, as can be seen for the 700 and 1000 eV cases.

Acknowledgment

This work was supported in part by the US Department of Energy, Office of Fusion Energy, Grant No DE-FG03-84ER52110, with UCLA.

References

[1] Sigmund P I 1969 *Phys. Rev.* **184** 383
[2] Winterbon K B, Sigmund P and Saunder J P 1968 *Dan. Vidensk. Selsk. Mat. Fys. Medd.* **36** 1
[3] Biersack J P and Haggmark L H 1980 *Nucl. Instrum. Methods* **174** 257
[4] Chou S P and Ghoniem N M 1983 *J. Nucl. Mater.* **117** 55
[5] Chou S P and Ghoniem N M 1987 *Nucl. Instrum. Methods* B **28** 175
[6] Hayward W H and Wolter A R 1969 *J. Appl. Phys.* **40** 2911
[7] Shapiro M H and Tombrello T A 1987 *Nucl. Instrum. Methods* B **18** 355
[8] Weller M R and Tombrello T A 1980 *Radiat. Eff.* **49** 239
[9] Libbrecht K G, Griffith J E, Weller R A and Tombrello T A 1980 *Radiat. Eff.* **49** 195
[10] Jakas M M and Harrison D 1986 *Nucl. Instrum. Methods Phys. Res.* B **14** 535
[11] Garrison B J, Winograd N, Deaven D M, Reimann C T, Lo D Y, Tombrello T A, Harrison D E and Shapiro M H 1988 *Phys. Rev.* B **37** 37
[12] Garrison B J, Walzl K, El-Maazawi M, Winograd N, Reimann C T and Deaven D M 1989 *Radiat. Eff. Defects Solids* **109** 287
[13] Reimann C T, El-Maazawi M, Walzl K, Garrison B J, Winograd N and Deaven D M 1989 *J. Chem. Phys.* **90** 2027
[14] Harrison D E Jr, Warren L G and Effron M H *J. Math. Phys.* **10** 1179
[15] Harrison D E Jr, Avouris P and Walkup R 1987 *Nucl. Methods Phys. Res.* B **18** 349
[16] Garrison B J, Winograd N, Lo D Y, Tombrello T A, Shapiro M H and Harrison D E Jr 1987 *Surf. Sci.* **180** L129
[17] Smith R, Harrison D E Jr and Garrison B J *Phys. Rev.* B **40** 93
[18] Maboudian R, Postawa Z, El-Maazawi M, Garrison B J and Winograd N *Phys. Rev.* B **42** 7311
[19] Chou S P and Ghoniem N M 1991 *J. Nucl. Mater.* **176** 909
[20] Chou S P and Ghoniem N M *Phys. Rev.* B **43** 2490
[21] Ziegler J F, Biersack J P and Littmark U 1985 *The Stopping and Range of Ions in Solids* (New York: Pergamon) p 48
[22] Foiles S M 1985 *Phys. Rev.* B **32** 7685
[23] Daw M S and Baskes M I 1983 *Phys. Rev. Lett.* **50** 1285
[24] Daw M S and Baskes M I 1984 *Phys. Rev.* B **29** 6443
[25] Greene J E and Barnett S A 1983 *J. Vac. Sci. Technol.* **21** 285
[26] Greene J E, Motooka T, Sundgren J E, Lubben D, Gorbatkin S and Barnett S A 1987 *Nucl. Instrum. Methods Phys. Res.* B **27** 226
[27] Hasan M A, Barnett S A, Sundgren J E and Greene J E 1987 *J. Vac. Sci. Technol.* A **5** 1883